

Co-conformational Variability of Cyclodextrin Complexes Studied by Induced Circular Dichroism of Azoalkanes

Bernd Mayer,^{*,†} Xiangyang Zhang,[‡] Werner M. Nau,^{*,‡} and Giancarlo Marconi^{*,§}

Contribution from the Institute for Theoretical Chemistry and Molecular Structural Biology, University of Vienna, UZAI, Althanstrasse 14, A-1090 Vienna, Austria, Department of Chemistry, University of Basel, Klingelbergstrasse 80, CH-4056 Basel, Switzerland, and Istituto di Fotochimica e Radiazioni d' Alta Energia, CNR Bologna, Via P. Gobetti 101, 40129 Bologna, Italy

Received December 19, 2000

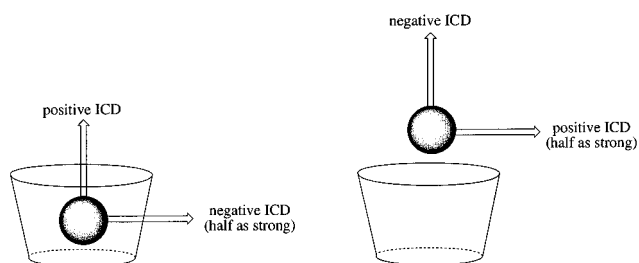
Abstract: The solution structures of the β -cyclodextrin complexes between 2,3-diazabicyclo[2.2.2]oct-2-ene (**1**) and its 1-isopropyl-4-methyl derivative **2** have been investigated by means of induced circular dichroism (ICD) and MM3-92 force-field calculations, which considered the effect of solvation within a continuum approximation. Of primary interest was the so-called co-conformation of the host–guest complex, i.e., the relative orientation of the guest within the host. A pool of low-energy complex structures, which were located by means of a Monte Carlo simulated annealing routine, was generated to evaluate the dynamic co-conformational variability of the complexes. The ICD effects were calculated for the computed low-energy structures by applying a semiempirical method. The experimental and theoretical ICD as well as the calculated low-energy complex geometries suggest solution co-conformations in which the parent compound **1** adapts a lateral arrangement with the ethano bridge of the guest penetrating deepest into the cavity and the azo group aligning parallel to the plane of the upper rim. In contrast, the alkyl derivative **2** prefers a frontal co-conformation with the isopropyl group penetrating deepest into the cavity and the azo group aligning perpendicular to the plane of the upper rim. The validity of the predictions of the Harata rule regarding the sign and the intensity of the ICD signals for the $n\text{-}\pi^*$, $n+\pi^*$, and $\pi\pi^*$ transition of the azo chromophore in dependence on the complex co-conformation are discussed. With respect to the co-conformational variability of the complexes of the two azoalkanes, it was observed that the nearly spherical guest **1** forms a geometrically better defined complex than the sterically biased, alkyl-substituted derivative **2**. This dichotomy is attributed to the largely different modes of binding for azoalkanes **1** and **2**. It is concluded that the goodness-of-fit in a host–guest complex cannot be directly related to the “tightness-of-fit”.

Introduction

In recent experimental studies simple aliphatic azo compounds have been exploited as probes for cyclodextrin (CD) host–guest complexes.^{1–4} In this context, the induced circular dichroism^{5–7} (ICD) due to the azo near-UV $n\pi^*$ absorption, which in contrast to symmetrical ketones is inherently symmetry-allowed,⁸ has provided a unique tool for structural assignments of the respective host–guest complexes *in solution*.

In contrast to the extensively employed larger aromatic probes,^{9–14} the azo chromophore ($-\text{N}=\text{N}-$) is sufficiently

Scheme 1



localized and small to allow a less ambiguous decision on whether the chromophore is located inside or outside the CD cavity. This is crucial to test the rules^{9,12,15} which have been developed for the prediction of the intensities and in particular signs of ICD effects, in particular the Harata⁹ and Kodaka¹⁵ rules, which refer to chromophores situated inside or outside the cavity, respectively. Scheme 1 shows the predictions of these rules with respect to the relative magnitude and sign of the ICD effect as a function of the direction of the electric dipole transition moment (arrows).

[†] University of Vienna. E-mail: bernd.mayer@univie.ac.at.

[‡] University of Basel. E-mail: werner.nau@unibas.ch.

[§] CNR Bologna. E-mail: marc@frae.bo.cnr.it.

(1) Krois, D.; Brinker, U. H. *J. Am. Chem. Soc.* **1998**, *120*, 11627–11632.

(2) Nau, W. M.; Zhang, X. *J. Am. Chem. Soc.* **1999**, *121*, 8022–8032.

(3) Zhang, X.; Nau, W. M. *Angew. Chem., Int. Ed.* **2000**, *39*, 544–547.

(4) Bobek, M. M.; Krois, D.; Brinker, U. H. *Org. Lett.* **2000**, *2*, 1999–2002.

(5) Connors, K. A. *Chem. Rev.* **1997**, *97*, 1325–1357.

(6) Rekharsky, M. V.; Inoue, Y. *Chem. Rev.* **1998**, *98*, 1875–1917.

(7) Zhdanov, Y. A.; Alekseev, Y. E.; Kompantseva, E. V.; Vergeichik, E. N. *Russ. Chem. Rev.* **1992**, *61*, 563–575.

(8) Nau, W. M. *EPA Newsletter* **2000**, *70*, 6–29.

(9) Harata, K.; Uedaira, H. *Bull. Chem. Soc. Jpn.* **1975**, *48*, 375–378.

(10) Shimizu, H.; Kaito, A.; Hatano, M. *Bull. Chem. Soc. Jpn.* **1979**, *52*, 2678–2684.

(11) Shimizu, H.; Kaito, A.; Hatano, M. *Bull. Chem. Soc. Jpn.* **1981**, *54*, 513–519.

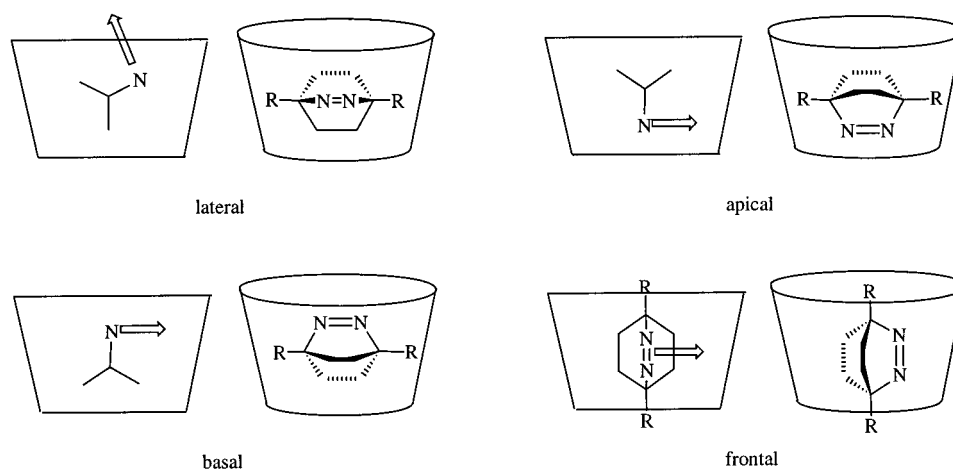
(12) Kajtár, M.; Horváth-Toró, C.; Kuthi, É.; Szejtli, J. *Acta Chim. Acad. Sci. Hung.* **1982**, *110*, 327–355.

(13) Kamiya, M.; Mitsunashi, S.; Makino, M.; Yoshioka, H. *J. Phys. Chem.* **1992**, *96*, 95–99.

(14) Kodaka, M. *J. Phys. Chem. A* **1998**, *102*, 8101–8103.

(15) Kodaka, M. *J. Am. Chem. Soc.* **1993**, *115*, 3702–3705.

Scheme 2



In a previous communication,³ it was observed that the closely related azoalkanes **1** and **2** form 1:1 inclusion complexes with β -CD with association constants of about 1000 M^{-1} for both guests in aqueous solution. A variety of experimental techniques, namely fluorescence, UV, 2D-ROESY NMR, and induced circular dichroism (ICD), were employed. Most importantly, different signs and intensities of the ICD bands due to the $n\pi^*$ azo absorption near 370 nm suggested a dramatic change in the complexation geometries in solution.



Different relative orientations of the constituents of supramolecular assemblies, including host–guest complexes, have been referred to as co-conformations to differentiate from the usual conformation which strictly refers to structural variations related to rotations of covalent bonds.¹⁶ The four principal co-conformations of azoalkanes **1** and **2** in cyclodextrin have been referred to as lateral, apical, basal, and frontal (Scheme 2). Among these, the first one was assigned to the β -CD•**1** complex and the last one to the β -CD•**2** complex.

The assignments were based on Harata's rule (left in Scheme 1), which predicts a positive ICD signal for a chromophore with its electric dipole transition moment aligned parallel to the axis of the cyclodextrin, and a negative one for a perpendicular orientation. The observed ICD effects, the positive for azoalkane **1** and the negative for **2**, were in agreement with this rule, because the electric dipole transition moment of the azo $n\text{-}\pi^*$ transition (near 370 nm) points along the azo π system,³ providing a nearly parallel alignment of the electric dipole transition moment for **1** and a perpendicular orientation for **2** (arrows in Scheme 2). The clear-cut assignments were facilitated by the circumstances that the lateral co-conformation for **1** is the only one with an anticipated positive ICD effect, while the frontal one is the only sterically feasible one for **2**.

The present contribution provides a comprehensive comparison of experimental, theoretical, computational, and empirical data, including measurements and assignments of additional ICD bands in the far-UV (<250 nm), detailed force-field calculations, computations of ICD effects, and further tests of the validity of the suggested rules.^{9,12,15}

(16) Balzani, V.; Credi, A.; Raymo, F. M.; Stoddart, J. F. *Angew. Chem., Int. Ed.* **2000**, *39*, 3348–3391.

Theoretical Methods

Calculation of Low-Energy Complex Structures. The potential energy computations of the 1:1 complexes between the two guest molecules, azoalkane **1** and **2**, and the host β -cyclodextrin (β -CD) were performed by using Allinger's MM3-92 force field and a block diagonal matrix minimization method.¹⁷ The fully minimized reference structure of β -CD, derived from crystallographic data,¹⁸ gave rise to a calculated energy of $71.3 \text{ kcal mol}^{-1}$, while the potential energies of azoalkane **1** and **2** were found to be 17.32 and $20.95 \text{ kcal mol}^{-1}$. These reference structures were used in subsequent calculations.

Low-energy complex geometries were located by employing a Monte Carlo simulated annealing (MCSA) routine^{19,20} within the program package MultiMize.²¹ Both potential energies (calculated by the force field) and solvation effects (calculated by a continuum approximation assigning atomic solvation parameters σ_j to the solvent accessible molecular surface area A_j) were considered within a modified Metropolis criterion, which has been shown to provide reliable structural data for cyclodextrin complexes in aqueous solution.^{22–24} Note that the inclusion of solvation effects, in particular hydrophobic interactions, is a prerequisite to obtain correct complex geometries.²³ The total solvation energies, computed via the continuum approximation by applying the Wesson–Eisenberg solvation parameter set,²⁵ were $-50.31 \text{ kcal mol}^{-1}$ for β -CD and 2.67 and $3.93 \text{ kcal mol}^{-1}$ for azoalkanes **1** and **2**, respectively.

The start geometry of each MCSA run was defined by a random relative orientation of host and guest molecule within a distance of 5 \AA . In each MCSA step this relative position of the individual host and guest is stochastically altered by a maximum of 0.5 \AA in x , y , and z coordinate, the guest molecule is rotated by a maximum of 5° , and the individual glucose units within the host molecule are also rotated by a maximum of 5° . Each stochastically generated structure is fully minimized within the force field and accepted according to the extended Metropolis criterion,²³ i.e., including both potential and solvation energies. The simulation temperature was kept constant at 300 K and low-energy complex structures were obtained within 5000 MCSA steps.

The potential energy gain ΔE_p (in kcal mol^{-1}) due to complex formation was obtained as the difference of the calculated potential

(17) Allinger, N. L.; Yuh, Y. H.; Lee, J. H. *J. Am. Chem. Soc.* **1989**, *111*, 8551–8566.

(18) Betzel, C.; Saenger, W.; Hingerty, B. E.; Brown, G. M. *J. Am. Chem. Soc.* **1984**, *106*, 7545–7557.

(19) Metropolis, N.; Rosenbluth, A. W.; Rosenbluth, M. B.; Teller, A. H.; J. *Chem. Phys.* **1953**, *21*, 1087–1092.

(20) Kirkpatrick, S.; Gelatt, C. D.; Vecchi, M. P. *Science* **1983**, *220*, 671–680.

(21) "MultiMize" Mayer, B., University of Vienna, 1997.

(22) Marconi, G.; Mayer, B.; Klein, C. T.; Köhler, G. *Chem. Phys. Lett.* **1996**, *260*, 589–594.

(23) Mayer, B.; Klein, C. T.; Marconi, G.; Köhler, G. *J. Inclusion Phenom. Mol. Recognit. Chem.* **1997**, *29*, 79–93.

(24) Mayer, B.; Klein, C. T.; Topchieva, I.; Köhler, G. *J. Comput. Aided Mol. Des.* **1999**, *13*, 373–383.

(25) Wesson, L.; Eisenberg, D. *Protein Sci.* **1992**, *1*, 227–235.

energies E_P of the complex and the sum of the isolated host and guest molecules. Similarly, the gain in solvation energy upon complexation (ΔE_S) was obtained as the difference in solvation energy (E_S) of the complex and the isolated molecules. The total complexation energy (E_C) corresponds to the sum of ΔE_P and ΔE_S .

Calculation of the Induced Circular Dichroism (ICD). The ICD of the host–guest complexes was calculated to allow a comparison of theoretically expected and experimentally observed spectroscopic data and, thus, to reassure the reliability of the computed low-energy structures. The theory of induction of optical activity for a chromophore included in a chiral host predicts the possibility of three different mechanisms.²⁶ The first mechanism (one electron) derives from the interaction of the electric and magnetic dipole transition moments of the chromophore and turns out to be zero for an achiral guest or very small in the case of state mixing due to the electrostatic field of the macrocycle. The second mechanism (dipole–dipole, d–d) arises from the interaction of the electric dipole transition moments of the guest excited states with the higher energy ones of the macrocycle. A convenient expression for the calculation of this term has been derived by Tinoco²⁷ by replacing the original dipole–dipole interaction scheme in the Kirkwood equations by the polarizability of the bonds of the chiral macrocycle. According to this approximation, the rotatory strength (R) for a transition $0 \rightarrow a$ is given by eq 1,

$$R_{0a} = \pi v_a \mu_{0a}^2 \sum_j \frac{v_{0j}^2 (\alpha_{33} - \alpha_{11})_j (GF)_j}{c(v_{0j}^2 - v_a^2)} \quad (1)$$

with

$$(GF)_j = \frac{1}{r_j^3} \left[\mathbf{e}_{0a} \mathbf{e}_j - \frac{3(\mathbf{e}_{0a} \mathbf{r}_j)(\mathbf{e}_j \mathbf{r}_j)}{r_j^2} \right] \mathbf{e}_{0a} \times \mathbf{e}_j \mathbf{r}_j$$

where \mathbf{e}_{0a} and \mathbf{e}_j are unit vectors along the transition moment μ_{0a} and parallel to the j th bond, respectively; v_{0j} and v_a are the frequencies of the electric transitions of the host and the guest, which are located at a distance \mathbf{r}_j , and α_{11} and α_{33} represent the bond polarizabilities at zero frequency, parallel and perpendicular to the symmetry axis of the bond j . In the present work the energies and electric moments in eq 1 were calculated by using the semiempirical quantum mechanical method CNDO/S, which is particularly well parametrized for the calculation of electronic transition energies. GF denotes the geometrical factor, which is based on the actual co-conformation of the host–guest complex and derived from a force-field optimization (cf. previous section).

In principle, a third mechanism can be operative which involves the magnetic dipole transition moment (m) of the chromophore and the electric dipole moment (μ) of the host. This so-called $m-\mu$ term is considered particularly important for symmetry-forbidden or weakly allowed $n\pi^*$ transitions⁴ and has been invoked to reproduce adequately the CD of carbonyls²⁶ and peptides.²⁸ Following the formulation of Schellman,²⁶ the ratio between the d–d and the $m-\mu$ terms is independent of the geometric factor GF and can be expressed by eq 2:

$$\frac{R_{0a}(d-d)}{R_{0a}(m-\mu)} = \sum_i \frac{v_a v_i}{v_a + v_i} hc \frac{R_{21} \mu_a \times \mu_i}{\mu_i \times m_a} \quad (2)$$

where R_{21} represents the host–guest distance, the index a stands for the excited state of the guest, and i refers to the far-UV excited states of the macrocycle. By combining the calculated energies and electric dipole moments of β -CD with the magnetic moment of the first $n-\pi^*$ excited state of compounds **1** and **2** (calculated within the framework of complete angular momentum),²⁹ one obtains in these cases values around 10 for the ratio in eq 2. Accordingly, the dipole–dipole term dominates by far and it is justified to approximate the total ICD through eq 1.

Note that the overall computational method consists of two steps: In the first step extended MCSA runs are performed by applying a co-optimization of potential energies and free energies of solvation within the Metropolis criterion and every accepted structure is stored, resulting in a pool of low-energy structures. In the second step the ICD spectra of these structures are individually computed by eq 1 and compared with the experimental spectra.

Experimental Section

Materials. Azoalkanes **1** and **2** were synthesized according to the reported procedures.^{3,30} They were first purified by sublimation, followed by recrystallization in *n*-hexane. β -Cyclodextrin was purchased from Fluka and used without purification. Deuterium oxide (>99.8%) was obtained from Glaser AG, Basel, Switzerland. UV spectra were obtained with a Perkin-Elmer Lambda 19 spectrophotometer (0.1 nm resolution).

Circular Dichroism Measurements. The reported ICD spectra were obtained with a Jasco J-720 spectropolarimeter (2-channel mode). To ensure the presence of the various ICD bands, spectra were also recorded on a different circular dichrograph (62A DS AVIV Circular Dichroism Spectrometer), at different concentrations, and at different path lengths: (a) 4 mM azoalkane and 12 mM β -cyclodextrin in a 10 mm cell, (b) 0.8 mM azoalkane and 3.2 mM β -cyclodextrin in a 10 mm cell, and (c) 4 mM azoalkane and 12 mM β -cyclodextrin in a 1 mm cell. These solutions were particularly suitable for sensitive measurements between 250 and 410 nm (OD ca. 0.3), 250–200 nm (OD ca. 0.5) and below 200 nm (OD ca. 0.5), respectively, where they displayed significant, yet not too high absorbance (<0.6). The interior of the spectrometer was thoroughly flushed with nitrogen before use. $\Delta\epsilon$ values were calculated as $\Delta\epsilon = \theta/(32982 \times L \times C)$,³¹ where L is the path length of the cell and C the concentration of complexed guest, calculated by employing the known binding constants.

Results

UV Absorption and ICD Spectra. The UV spectra of azoalkanes **1** and **2** are shown in Figure 1a. The weak band in the near-UV (ca. 370 nm) is characteristic for bicyclic azoalkanes and can be assigned to the $n-\pi^*$ transition (antisymmetric combination of the two nitrogen lone pairs), while the stronger band at ca. 195 nm can be assigned to a $\pi\pi^*$ excitation. The corresponding $n+\pi^*$ transition (symmetric combination of the two nitrogen lone pairs) is presumed to lie below the rising $\pi\pi^*$ band at ca. 220 nm. Although it is symmetry forbidden, it may borrow intensity from the close-lying, strongly allowed $\pi\pi^*$ transition. Several indications support the position of the $n+\pi^*$ transition: (a) Calculations predict the $n+\pi^*$ transition at lower energy than $\pi\pi^*$ (see below). (b) Gas-phase UV spectra reveal a discrete fine structure in the on-set of the far-UV band, which would be expected for a vibronically induced (forbidden) $n+\pi^*$ band. (c) Protonation of azoalkane **1** (in 1 M H_2SO_4 , cf. $pK_a = 0.5$)³² shifts the $n\pi^*$ absorption band to ca. 310 nm, about halfway in energy between the $n-\pi^*$ and the presumed $n+\pi^*$ band. Since the degeneracy of the azo lone pairs is lifted upon protonation, the energy of the resulting band can be taken as a crude approximation for the basis energies of the nitrogen lone pairs. (d) The present ICD spectra reveal distinct features in the presumed region, which cannot be accounted for in terms of a single transition in the far-UV.

Figure 1b shows the experimental ICD spectra of the β -CD•**1** and the β -CD•**2** complex from 190 to 410 nm. For azoalkane **1**, a positive ICD band due to the $n-\pi^*$ transition is observed and a weak negative band at ca. 220 nm, which is assigned to

(26) Schellman, J. A. *Acc. Chem. Res.* **1968**, *1*, 147–151.

(27) Tinoco, I. Jr. *Adv. Chem. Phys.* **1962**, *4*, 113–160.

(28) Woody, R.; Tinoco, I. *J. Chem. Phys.* **1967**, *46*, 4927–4945.

(29) Hezemans, A. M. F.; Obbink, J. H. *Theor. Chim. Acta* **1976**, *43*, 75–87.

(30) Askani, R. *Chem. Ber.* **1965**, *98*, 2551–2555.

(31) Rodger, A.; Nordén, B. *Circular Dichroism and Linear Dichroism*; Oxford University Press Inc.: New York, 1997.

(32) Nelsen, S. F.; Petillo, P. A.; Chang, H.; Frigo, T. B.; Dougherty, D. A.; Kafarty, M. *J. Org. Chem.* **1991**, *56*, 613–618.

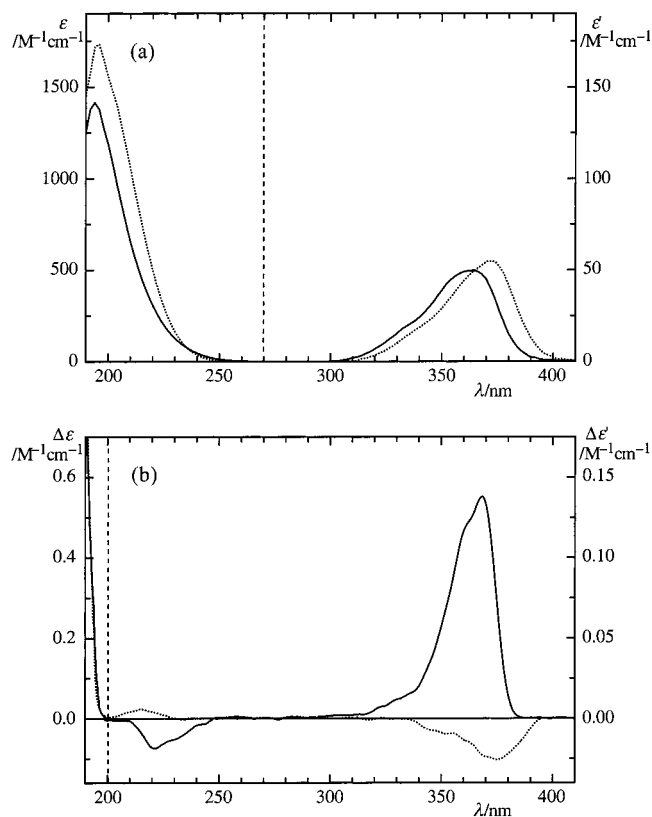


Figure 1. (a) Experimental UV absorption spectra of water solutions containing 4.0 mM azoalkane **1** (solid line) or **2** (dashed line). (b) Normalized ICD spectra of water solutions containing 4.0 mM azoalkane **1** (solid line) or **2** (dashed line) in the presence of 12.0 mM β -CD. The ordinate labeling on the left of both graphs refers to the regions left of the dashed line, which were recorded in a 1 mm cuvette, and that on the right to the regions right of the dashed line, which were recorded in a 10 mm cuvette.

the $n+\pi^*$ transition. In contrast, azoalkane **2** shows a negative ICD signal in the near-UV (assigned to the $n-\pi^*$ transition) and a very weak positive band at ca. 210 nm (assigned to the $n+\pi^*$ transition). With respect to the absolute ICD intensities of the bands around 370 and 220 nm, the positive ICD of β -CD·**1** is about 4 times stronger than the negative ICD of β -CD·**2** and the negative ICD of β -CD·**1** is also about 3 times stronger than the positive ICD of β -CD·**2**.

Structure Calculations. The low-energy structures of the 1:1 complexes between β -CD and azoalkanes **1** and **2** were located by means of a Monte Carlo simulated annealing (MCSA) routine in the MM3-92 force field and include solvation energies obtained by a continuum approximation. Table 1 gives the factorized potential and solvation energy contributions for the four different co-conformations depicted in Scheme 2. Four different energy contributions (van der Waals, dipole–dipole, bending, and torsion) favor the lateral inclusion. Most interesting, although the guest is virtually spherical, steric contributions from the strain of the host, in particular bending and torsion energy terms, are large and favor the lateral co-conformation by ca. 3–6 kcal mol⁻¹, in addition to the van der Waals and dipole–dipole interactions, which contribute another 1 kcal mol⁻¹ stabilization. Moreover, both the hydrophobic as well as the hydrophilic contributions lower the solvation energy term for the lateral co-conformation by ca. 1 kcal mol⁻¹ each. This decrease in solvation suggests a deeper inclusion of the guest for the lateral co-conformation.

Azoalkane **1** is found to be completely immersed into β -CD and adapts a central position in the cavity. A typical low-energy

Table 1. Factorized Potential and Solvation Energies (in kcal mol⁻¹) for β -CD·**1** Complexes with Lateral, Frontal, Apical, and Basal Co-conformation (see Scheme 2)

contributions	lateral	frontal	apical	basal
force field energies (MM3/92)				
total (E_P)	73.60	80.88	78.80	78.49
compression	6.59	6.65	6.56	6.51
van der Waals	65.88	66.77	66.01	65.96
dipole–dipole	–33.64	–32.68	–33.15	–33.06
bending	30.95	33.45	31.84	31.73
stretch–bend	1.96	1.97	1.95	1.91
torsion	3.36	6.09	6.99	6.83
bend–bend	–0.09	–0.04	–0.10	–0.10
torsion–stretch	–1.31	–1.32	–1.30	–1.30
solvation energies (continuum approximation)				
total (E_S)	–49.98	–48.10	–49.17	–49.33
phobic solvation	6.58	7.05	6.77	6.93
philic solvation	–56.56	–55.15	–55.93	–56.26

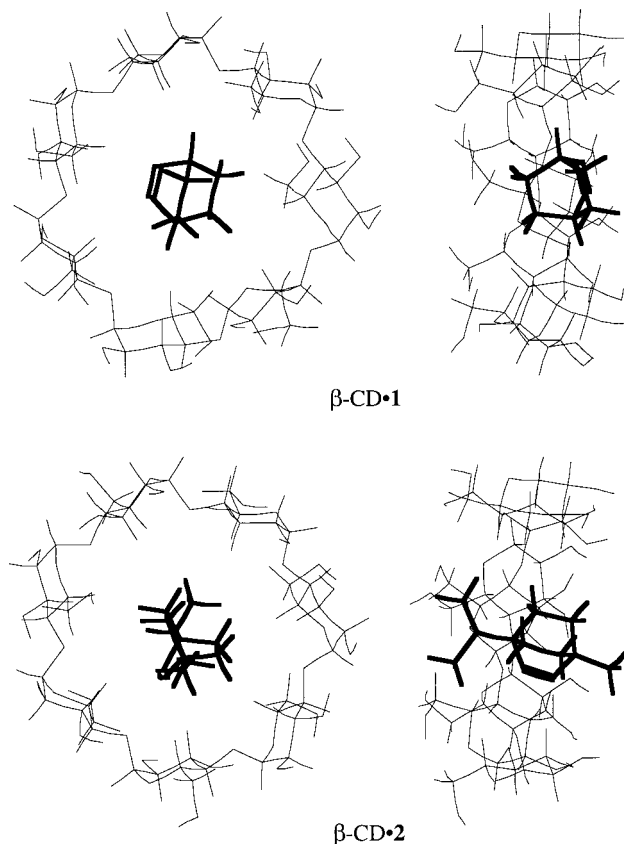


Figure 2. Representative low-energy structures of the host–guest complexes between β -CD and azoalkanes β -CD·**1** and β -CD·**2**. Shown is a frontal view of the secondary hydroxyl rim side (left) and after rotation by about 90° (right). The specific energetic and structural data for β -CD·**1** are given in Table 1 (lateral co-conformation) and those for β -CD·**2** are as follows: $E_P = 65.48$ kcal mol⁻¹, $E_S = -46.72$ kcal mol⁻¹, $\Delta E_P = -26.77$ kcal mol⁻¹, $\Delta E_S = -0.34$ kcal mol⁻¹, $E_C = -27.11$ kcal mol⁻¹, $d = 0.58$ Å, $\alpha = 68.10^\circ$.

structure is given in Figure 2. The data for the lateral co-conformation in Table 1 refer to the left structure in this figure. Although azoalkane **1** can be effectively considered as a spherical molecule, the azo bridge displays a strong preference for orienting parallel to the upper cyclodextrin rim, i.e., the plane defined by the glycosidic oxygens. The computed gain in potential energy, ΔE_P , is -15.02 kcal mol⁻¹ and that in solvation energy, ΔE_S , is -2.34 kcal mol⁻¹, which results in a total complexation energy, E_C , of -17.36 kcal mol⁻¹.

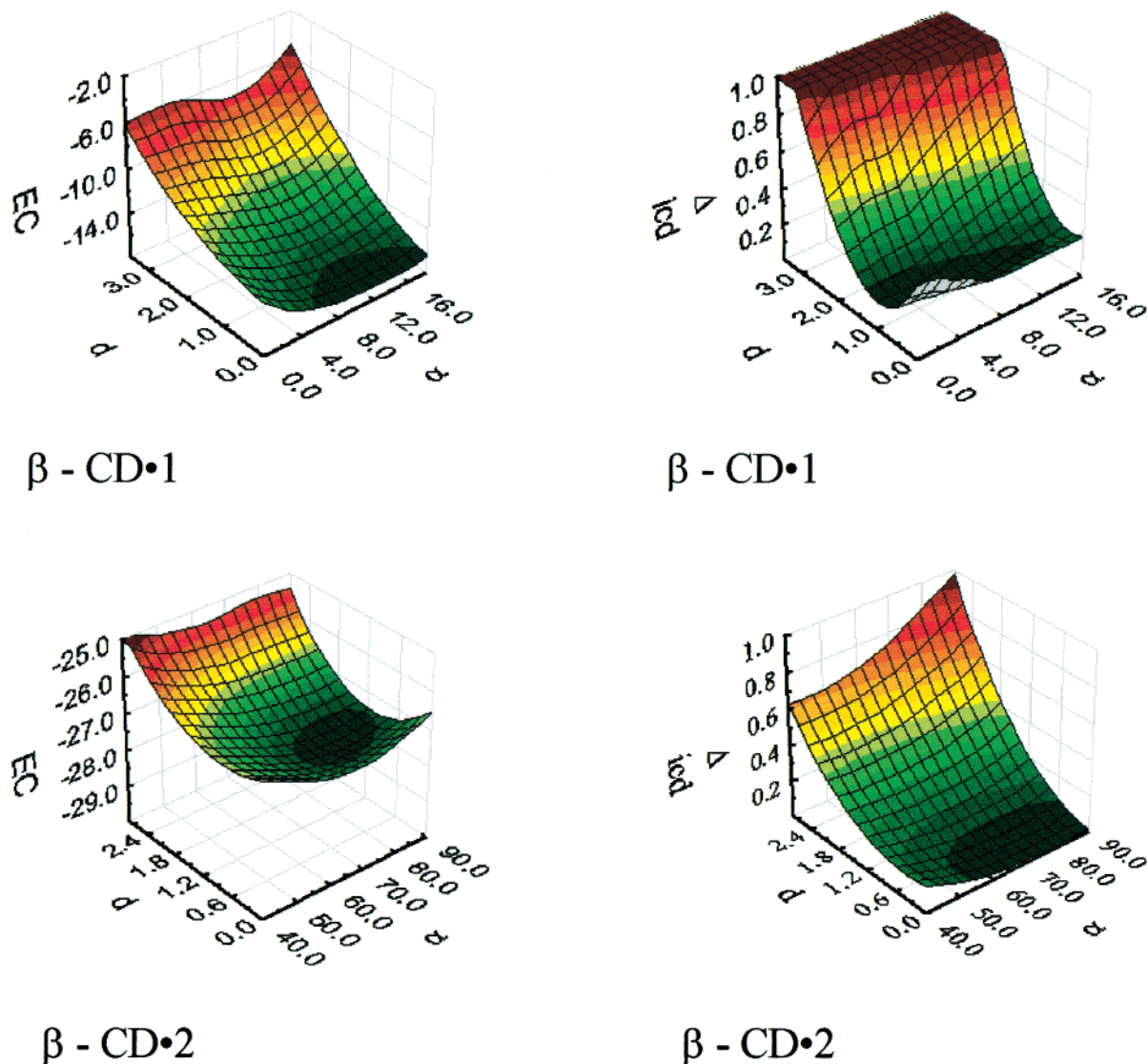


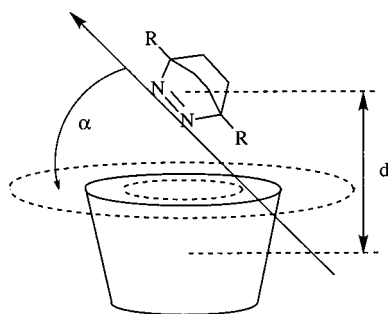
Figure 3. Surfaces for the color-coded complexation energy (E_C) and the color-coded deviation between calculated and experimental ICD (ΔICD) of the host–guest complexes $\beta\text{-CD}\cdot\mathbf{1}$ (upper) and $\beta\text{-CD}\cdot\mathbf{2}$ (lower) as a function the host–guest distance d in Å and the relative tilt angle α in deg. The surfaces were obtained by means of a cubic-spline interpolation through the data for 1000 low-energy structures. Note the large difference of the α scale in the upper and lower plots.

A perpendicular alignment of the azo bridge with respect to the cyclodextrin axis as observed for azoalkane **1** is sterically obstructed for azoalkane **2**. Figure 2 shows a typical low-energy complex structure, in which the azo bridge adapts an orthogonal position with respect to the upper rim, i.e., the plane defined by the glycosidic oxygen atoms of the host. Despite this rotation of the azo group by about 90° , azoalkane **2** is also fully included and resides in a central position of the cavity. The gain in potential energy, ΔE_p , of -26.77 kcal mol $^{-1}$, along with a small gain in solvation energy, ΔE_s , of -0.34 kcal mol $^{-1}$, provides a total complexation energy, E_C , of -27.11 kcal mol $^{-1}$. Both the $\beta\text{-CD}\cdot\mathbf{1}$ and the $\beta\text{-CD}\cdot\mathbf{2}$ complex are stabilized by contributions from potential as well as solvation energy. However, the total complexation energy for azoalkane **2** is about 10 kcal mol $^{-1}$ lower, indicating an increased stability. This finding, however, is not supported by the experimentally determined association constants, which give values of ca. 1000 M $^{-1}$ for both complexes in water.³ This contrast, which is presumably due to the approximations in the continuum solvation model, limits the use of the computational method for predicting absolute complexation energies, while the geometries have been previously shown to be in excellent agreement.^{22–24}

In another generic arrangement of **2** in $\beta\text{-CD}$ the methyl rather than the isopropyl substituent is situated near the primary hydroxyl rim side of $\beta\text{-CD}$ (i.e., a 180° rotation of the guest with respect to the structure given in Figure 2). However, complexes of this type gave significantly higher (>10 kcal mol $^{-1}$) complexation energies and were not further considered in the following analysis.

The representative structures in Figure 2 are arbitrarily taken from a large pool of 1000 low-energy structures computed within the MCSA runs for each complex. The left-hand plots in Figure 3 show the color-coded complexation energies E_C as a function of the host–guest distance (d) in Å and the tilt angle (α) in the cavity. As shown in Scheme 3, the distance d was defined as the center of mass distance between guest and $\beta\text{-CD}$ and α was taken as the angle between the axis pointing along the azo bond and the upper cyclodextrin rim, i.e., the plane defined by the glycosidic oxygens.²³ The 3D energy hypersurfaces for azoalkanes **1** and **2** in Figure 3 were obtained by a cubic-spline interpolation through the 1000 low-energy complex structures, which were obtained in the MCSA runs and for each of which the respective structural parameters d and α were recorded. For example, α in Figure 2 is close to 0° for the

Scheme 3



β -CD•**1** complex, but about 90° for the β -CD•**2** complex. The importance of this angle lies in the fact that it defines the relative orientation of the electric dipole transition moment, which is required for the prediction of the sign of ICD effects.

As follows from Figures 2 and 3, the host–guest distances are small for both complexes (0–1.5 Å), which characterizes them as fully immersed 1:1 inclusion complexes. This is in agreement with experimental data.^{2,3} However, the two complexes display a dramatic, unprecedented variation in the co-conformation of the guest and the host, which can be studied in terms of the tilt angle α . Interesting in this respect is not only the fact that the tilt angle of the β -CD•**2** complex is large as a consequence of steric constraints imposed by the substituents, but also that it displays a large distribution of nearly isoenergetic structures (near -27 kcal mol⁻¹, green region in the lower left plot of Figure 3) with α ranging from 60 to 90° . Obviously, the complexed azoalkane **2** is quite flexible with respect to the tilt. In contrast, the low-energy β -CD•**1** complexes display not only very small tilt angles near 0° , but their range is highly restricted from 4 to 16° (green region in the upper left plot of Figure 3; note the difference in the upper and lower α scale).

Induced Circular Dichroism (ICD). The calculation of ICD spectra of the host–guest complexes and comparison with experimental spectra provides a powerful test of the computed structural data. The UV spectral calculations place the $n_{-}\pi^*$ transition of azoalkanes **1** and **2** at ca. 400 nm, the $n_{+}\pi^*$ transition at ca. 240 nm, and the $\pi\pi^*$ transition below 200 nm, in agreement with the assignments of the UV-spectral data. The oscillator strengths for the isolated, undistorted compounds are calculated as 0.002 for $n_{-}\pi^*$, 0 for $n_{+}\pi^*$, and 0.8 for $\pi\pi^*$. The computed data reveal that the alkyl substitution in **2** is only a weak perturber of the electronic transitions of the azo chromophore, as is found experimentally (Figure 1a).

Figure 4 shows computed ICD spectra of the low-energy structures given in Figure 2, i.e., for β -CD•**1** and β -CD•**2**. The computation predicts correctly the sign and relative intensity of the ICD due to the $n_{-}\pi^*$ and $n_{+}\pi^*$ bands. The experimental difference in absolute intensity of the $n_{-}\pi^*$ ICD signal (factor 4–5) is more pronounced than the computed one (factor 2). The latter is in fact also expected on the basis of the Harata rule, which applies for deep inclusion complexes (left in Scheme 1). On the other hand, the calculation predicts a 2–3 times stronger ICD for the $n_{+}\pi^*$ band of β -CD•**2** compared to β -CD•**1** (Figure 4) while experimentally the reverse intensity ratio is found (ICD effects at ca. 220 nm, Figure 1b). The differences in the absolute intensities of the theoretical ICD (calculated for the specific structures in Figure 2) and the experimental spectra cannot be due to differences in the binding constants, which are essentially the same for both azoalkanes (ca. 1000 M⁻¹).³ Presumably, they are related to the fact that the experimental ICD reflects a Boltzmann-weighted distribution

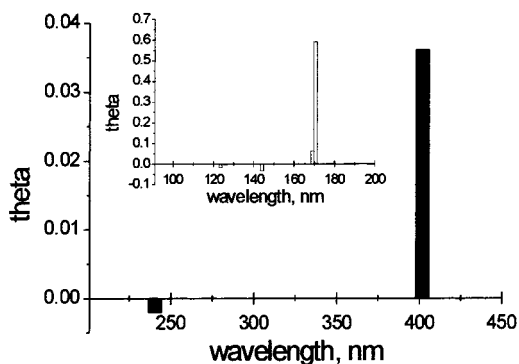
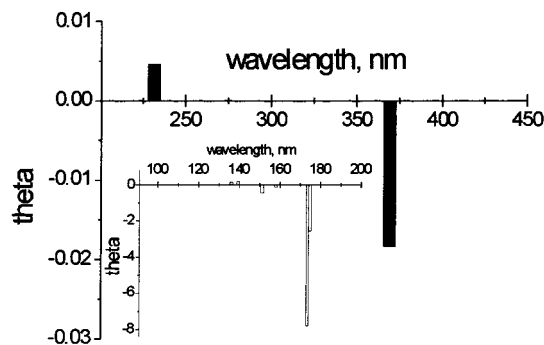
 β -CD•**1** β -CD•**2**

Figure 4. Calculated ICD spectra of the β -CD•**1** and β -CD•**2** structures given in Figure 2.

of the ICD contributions of all energetically accessible complex structures. A further theoretical analysis along this line was not attempted since we do not consider the calculated absolute ICD intensities sufficiently accurate at present to reproduce experimental intensities.

It should be noted that the $n_{+}\pi^*$ transition in the β -CD complex is calculated to have some oscillator strength (0.001) as well as rotational power, which may derive from intensity borrowing from the strong, high-energy $\pi\pi^*$ transition and also from the loss of local symmetry in the complex. This rationalizes the presence of a small ICD signal in the corresponding region of the spectrum (Figure 1b). The $\pi\pi^*$ absorption bands are predicted at significantly shorter wavelengths than observed (insets in Figure 4). Unfortunately, although the ICD intensity of these bands is predicted to be very high, a further analysis and clear-cut assignment was not possible since neat β -CD solutions produce also a strong positive ICD signal in this high-energy region (<195 nm). In summary, the computational data suggest that the β -CD complexes of azoalkanes **1** and **2** should give rise to opposite ICD signals (different signs) of the $n_{-}\pi^*$ and $n_{+}\pi^*$ transitions. Moreover, the ICD effects of the $n_{-}\pi^*$ and $n_{+}\pi^*$ transitions should differ in their signs. These expectations are met by the experimental ICD spectra (Figure 1b).

The ICD analysis would be in agreement with the structures in Figure 2. However, each of these two structures is only one representative out of the calculated pool of 1000 local minima with low energies, i.e., with complexation energies E_C around -17 kcal mol⁻¹ for β -CD•**1** and -27 kcal mol⁻¹ for β -CD•**2**. Hence, it was of interest to examine all local minima, with varying host–guest distance and tilt angle, with respect to their agreement with the experimental ICD signals. This procedure allows one to define an ensemble of structures which are both

Table 2. Structural and Spectroscopic Characteristics of β -CD•1 Complexes with Lateral, Frontal, Apical, and Basal Co-conformation

parameter	lateral	frontal	apical	basal
d^a	0.83	0.92	1.53	1.14
α^b	3.70	78.92	2.22	1.80
ΔICD^c	0.01	0.86	0.64	0.51

^a Host–guest distance, in Å. ^b Tilt angle, in deg. ^c Normalized deviation of computed and experimentally determined ICD spectrum, cf. text.

energetically feasible and show consistent ICD signals, and it addresses the question of co-conformational variability of the solution-phase complexes. In practice, the deviation of the computed ICD from the experimentally determined spectrum, ΔICD , was calculated for each of the 1000 low-energy structures of both azoalkanes **1** and **2** (Figure 3). The mean deviation took into account the sign as well as the relative intensity of the bands and was then normalized in the interval [0,1]. A ΔICD value of 0 applies for the structure whose ICD fits the experimental spectrum best, and a value of 1 results for the structure with the worst similarity between calculated and experimental spectra. These normalized ICD deviations are plotted versus the host–guest distance (d) and tilt angle (α) in the right-hand plots of Figure 3, using again a cubic-spline interpolation through the entire pool of low-energy structures.

The overall agreement between the calculated energy hypersurfaces (left-hand plots in Figure 3) and the calculated deviations between theoretical and experimental ICD effects (right-hand plots in Figure 3) is excellent, thus providing confidence in the calculated solution structures. In the case of **2** a correct sign and relative intensity of the ICD (corresponding to a low ΔICD value) is computed for complexes with a host–guest distance below 1.3 Å and a tilt angle larger than 56°. For β -CD•1 correct ICD signals are found for d values between 0.3 and 1.5 Å, and a tilt angle interval of 0–10°. Interesting to note is the strict dependence of the ICD signal on the host–guest distance: a more peripheral inclusion for **1** ($d > 1.5$ Å) as well as **2** ($d > 1.3$ Å) gives rise to computed ICD spectra which show only poor agreement with the experiment. This is in fact the computed manifestation of the Harata and Kodaka rules (left and right in Scheme 1), which predicts an inversion of ICD signs when the chromophore moves from the inside to the outside of the host. Interestingly, however, in the case of azoalkane **1**, perfectly centered inclusion ($d = 0$ –0.3 Å) produces also a poor agreement with the experimental ICD data.

A more detailed assignment of the co-conformation was desirable for the complex of azoalkane **1**, for which four co-conformations need to be considered (Scheme 2). Table 2 gives structural data and ICD deviations for four local minima corresponding to each co-conformation. Since the frontal, basal, and apical co-conformations possess high energies and tend to convert into the lateral co-conformation during optimization, these calculations were only run for one representative structure (cf. Table 1) rather than on an ensemble of geometries as was possible for the lateral co-conformation. Note that the host–guest distance (d) indicates a slightly deeper inclusion for the lateral mode, which is, as noted above, also reflected by the decreased solvation energy of this complex type. The tilt angle α reflects again the alignment of the azo bond with respect to the upper rim. For example, a value of 90° should apply to the frontal co-conformation, which is altered to about 79° in the course of gradient optimization. Most importantly, the lateral co-conformation gives the best agreement with the experimental ICD, and since it is also by far the energetically most favorable

one, it is assigned to the solution structure, thus supporting the preliminary assignment.³

Discussion

A detailed knowledge of the solution co-conformations of weakly bound intermolecular host–guest complexes is of considerable interest for the understanding of enzyme–substrate interactions and the rational design of catalytically active supramolecular materials. The circular dichroism,^{31,33} which can be induced by a host or enzyme upon a guest or substrate or vice versa, if at least one component is optically active, can be employed to assess the co-conformations in the resulting host–guest complexes. In short, the sign and magnitude of this induced circular dichroism (ICD) depends, inter alia, on the relative direction of the electric dipole transition moments and, thus, represents a sensitive function of the molecular geometries, i.e., the co-conformation of the complex. In addition to the assessment of the averaged minimum co-conformations in dependence of structural modification of either the host or the guest, it is of interest to obtain information on the dynamics of the complexes, i.e., to assess the entire co-conformational space which is energetically accessible. The latter may be essential to evaluate the most favorable geometries for catalytic activity, which may not coincide with the energetically most favorable ones. Moreover, the co-conformational space accessible in solution may be much larger than that implied by crystallographic data.^{34,35}

In this work, we have examined the co-conformations and co-conformational variability of the host–guest complexes between azoalkanes **1** and **2** as guests and β -cyclodextrin as host. Cyclodextrins are natural, water-soluble host structures with known catalytic potential. The selected azoalkanes are advantageous model guest molecules due to their small molecular size, their water-solubility, and the characteristics of their azo chromophore, which is localized and possesses an inherent (not induced) electric dipole transition moment of its near-UV $n\pi^*$ absorption band. The latter is required for reliable co-conformational assignments based on ICD effects.

Co-conformational Assignments Based on Induced Circular Dichroism. The circular dichroism signals of azoalkanes **1** and **2** induced by β -CD through inclusion complex formation arise from the $n\pi^*$ transition near 370 nm and the $n+\pi^*$ transition near 220 nm. The latter is actually symmetry forbidden, but gains some rotational strength through the distortion occurring in the complex and intensity borrowing from the high-lying $\pi\pi^*$ state. The β -CD•1 complex gives rise to a positive ICD of the near-UV band, while the β -CD•2 complex produces a negative signal in this region. These signs of the ICD signals are in line with a lateral co-conformation for azoalkane **1** and a frontal one for azoalkane **2**.

Harata's rule should apply to deep inclusion complexes such as β -CD•1 and β -CD•2 (left in Scheme 1). This rule predicts a positive ICD in cyclodextrins, when the electric dipole transition moment of the guest is aligned parallel to the axis of the cyclodextrin, but a negative one for a perpendicular arrangement. Since the $n\pi^*$ transition moment of *cis*-azoalkanes points along the azo- π system (arrows in Scheme 2), a parallel arrangement obtains for a lateral co-conformation and a perpendicular one for the frontal one, thus accounting for the observed positive and negative ICD signals near 370 nm, the $n\pi^*$ transition

(33) Nakanishi, K.; Berova, N.; Woody, R. W. *Circular Dichroism: Principles and Applications*; VCH Publishers: New York, 1994; p 570.

(34) Harata, K. *Chem. Rev.* **1998**, *98*, 1803–1827.

(35) Saenger, W. In *Inclusion Compounds*; Atwood, J. L.; Davies, J. E. D., MacNicol, D. D., Eds.; Academic Press: London, 1984; Vol. 2.

(Figure 1). The predictions by this rule are also reflected in the ICD calculations for the $n\text{-}\pi^*$ bands of the respective complex geometries (Figure 4).

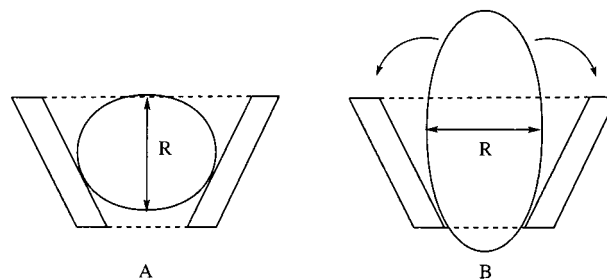
The assignments of a lateral co-conformation to **1** and a frontal one to **2** are strongly supported by the present force-field calculations, which predict these complexation modes to be favorable by more than 5 kcal mol⁻¹. This strong preference for one of the various inclusion geometries can be readily rationalized for derivative **2**, which is sterically biased toward a frontal inclusion, but is quite surprising for the parent compound **1**. First, azoalkane **1** is nearly spherical, such that interconversion between several nearly isoenergetic co-conformations is intuitively expected. Moreover, it is commonly assumed⁵ and confirmed for phenols^{36–38} and related polar aromatic compounds that the polar “side” of a molecule tends to interact more strongly with the aqueous phase, a presumption that is not met for a lateral co-conformation, in which a nonpolar ethano bridge, not the polar azo group, is situated near the aqueous outside.³⁹

The ICD effects observed for azoalkane **1** and **2** near 220 nm, the $n\text{-}\pi^*$ transition, are opposite to the corresponding $n\text{-}\pi^*$ bands and there is an agreement between the signs of the calculated and experimental ICD effects in this region. A simple analysis of the signs of these weaker bands in terms of the Harata rule is not feasible due to the fact that this transition is symmetry forbidden for the isolated molecule, i.e., the transition moment vanishes. The fact that optical activity of this band is nevertheless observed may be due to the geometrical distortion of the chromophore in the complex and also vibronic coupling with upper excited states.

An analysis of the signals below ca. 195 nm, including the $\pi\pi^*$ absorption band of these azoalkanes, was not feasible due to the strong circular dichroism produced by $\beta\text{-CD}$ itself in this region. Accordingly, while the complexes displayed also positive signals below 200 nm, it cannot be deconvoluted to which degree these bands stem from the circular dichroism of uncomplexed and complexed cyclodextrin (which may differ by an unknown amount) or from the actual induced circular dichroism upon the $\pi\pi^*$ band. Regardless of this experimental shortcoming, it is interesting to note that the ICD calculations predict the $\pi\pi^*$ transitions to display very strong (10 times stronger for **2**) ICD effects with the same signs as those of the $n\text{-}\pi^*$ bands. This result is not expected on the basis of the Harata rule since these two symmetry-allowed transitions have orthogonal transition moments (pointing along the azo bond in the case of $\pi\pi^*$) and should give rise to opposite ICD effects. Presumably, the opposite calculated signs for the far-UV transitions are due to the fact that they are heavily mixed with $\sigma\sigma^*$ transitions. Consequently, care must be taken when applying qualitative rules^{9,12,15} for predicting ICD effects of mixed high-energy electronic transitions.

Co-conformational Variability. Our computational study has revealed that the host–guest complex of azoalkane **1** has a significantly more restricted co-conformational space than that of azoalkane **2** (cf. Results and Figure 3). In particular, the

Scheme 4



$\beta\text{-CD}\cdot\mathbf{1}$ complex displays much smaller variations with respect to the tilt angle (α) than $\beta\text{-CD}\cdot\mathbf{2}$. Azoalkane **1** is nearly spherical and has a van der Waals diameter (R) of ca. 5 Å, while the derivative **2** is significantly elongated along one axis due to the alkyl groups (ca. 8 Å), but maintains its diameter in the orthogonal coordinates. Consequently, azoalkane **2** is more encumbered and sterically biased, such that the larger variability in the binding mode comes as some surprise. The intuitive anticipation that the spherical guest **1** can adapt a large number of energetically similar geometries, while the sterically encumbered derivative cannot, is *not* supported by the computed data. Apparently, structural bias in host–guest complexation, i.e., the preference for one particular co-conformation, does not necessarily reduce the degrees of orientational freedom in a host–guest complex.

We presume that azoalkane **1** acts essentially as a stopper or plug of the upper cyclodextrin cavity in the lateral arrangement (cf. co-conformation A in Scheme 4) with the ethano bridge providing an anchor against free rotation (cf. Scheme 2), thus precluding any major movements. In contrast, although azoalkane **2** appears to provide an equally good fit (judging on the basis of the host–guest distance, the complexation energy, and the binding constant), a tilting motion within the host (cf. co-conformation B in Scheme 4) is free to occur, resulting in the observed wide range in tilt angles (Figure 3). The interesting conclusion from our study is that the goodness-of-fit in a host–guest complex cannot be directly related to the “tightness-of-fit”, when largely different modes of binding apply as is the case for azoalkanes **1** and **2**.

Conclusions

Two different modes of complexation by $\beta\text{-cyclodextrin}$ have been realized for azoalkanes **1** and **2**, in which the azo chromophore has been aligned either parallel or perpendicular to the axis of the cyclodextrin. The co-conformations of the resulting host–guest complexes in aqueous solution have been analyzed by means of experimental and theoretical ICD effects and force field calculations. While the calculated absolute complexation energies and absolute ICD intensities cannot be directly compared with experimental data, the structural information of the calculations and the relative ICD intensities as well as the signs of the ICD effects provide mutually consistent results. The ICD analysis has further demonstrated that the rule of Harata for predicting the signs of ICD effects from the direction of the electric dipole transition moment appears to be applicable for the near-UV $n\text{-}\pi^*$ transition, but not for the high-energy transitions. Finally, the force-field calculations have provided an insight into the co-conformational variability of the host–guest complexes. Most importantly, the goodness-of-fit appears to be unrelated to variations in the orientational freedom of a host–guest complex, at least when the co-conformations are very different.

(36) Rüdiger, V.; Eliseev, A.; Simova, S.; Schneider, H.-J.; Blandamer, M. J.; Cullis, P. M.; Meyer, A. J. *J. Chem. Soc., Perkin Trans. 2* **1996**, 2119–2123.

(37) Marconi, G.; Monti, S.; Mayer, B.; Köhler, G. *J. Phys. Chem.* **1995**, 99, 3943–3950.

(38) Wood, D. J.; Hruska, F. E.; Saenger, W. *J. Am. Chem. Soc.* **1977**, 99, 1735–1740.

(39) Note that azoalkane **1** has a very large dipole moment of 3.5 D, which is directed perpendicular to the azo N=N bond and lies in the C–N=N–C plane: Harmony, M. D.; Talkington, T. L.; Nandi, R. N. *J. Mol. Struct.* **1984**, 125, 125–130.

Acknowledgment. This work was financially supported by the Swiss National Science Foundation within the National Research Program “Supramolecular Functional Materials” (grant No. 4047-057552). We would like to thank Prof. C. Bohne for independent measurements of some critical regions of the ICD spectra and for discussions regarding the co-conformational variability problem. W.M.N. thanks Prof. G. Greiner, University

of Stuttgart-Hohenheim, for discussions on the gas-phase spectra. G.M. appreciates many helpful discussions with Dr. D. Krois concerning the role of the mechanisms generating optical activity in related systems.

JA004295S